A predictive model for color pattern formation in the butterfly wing of *Papilio dardanus*

This paper is dedicated to Professor Masayasu Mimura on his sixtieth birthday.

Anotida Madzvamuse, Philip K. Maini, Andrew J. Wathen and Toshio Sekimura

Previously, we have proposed a mathematical model based on a modified Turing mechanism to account for pigmentation patterning in the butterfly wing of *Papilio dardanus*, well-known for the spectacular phenotypic polymorphism in the female of the species (Sekimura, *et al.*, Proc. Roy. Soc. Lond. **B 267**, 851–859 (2000)). In the present paper, we use our model to predict the outcome of a number of different types of cutting experiments and compare our results with those of a model based on different hypotheses.

1. Introduction

Pigmentation patterns on lepidopteran wings, which cover the whole dorsal and ventral wing monolayers, can be complicated in structure and they are sometimes used for identification of species. However, owing to the pioneering work of Schwanwitsch (1924) and Süffert (1927) on the nymphalid ground plan, the complicated patterns on the wings can be understood as a composite of a relatively small number of pattern elements (for details, see Nijhout, 1991). In spite of these simplifications, the problem of color pattern formation in wings is still not fully resolved and there exist few mathematical models to account for the diversity of color pattern in wings except for some specific features.

Among them, the development of eyespot patterns is the best understood mechanism at present. Nijhout (1990) presented a model for eyespot formation based on experimental evidence, in which a spatial distribution of sources and sinks of pattern organisers is firstly set up and the organising centers induce color patterns in their surroundings. Nijhout succeeded in producing point-like patterns in the exact locations of the organizing centers by an activator-inhibitor mechanism (Meinhardt, 1982) that assumes that the

wing veins act as fixed boundary conditions for the activator and as reflecting boundaries for the inhibitor (Nijhout, 1990, 1994).

Regarding global patterns covering the entire wing surface, Murray (1981) proposed a simple diffusion model for the development of the commonly observed crossbands of pigmentation shortly after pupation. Murray's model extends the idea of a determination stream proposed by Kühn and von Engelhardt (1933), namely, that the anterior and posterior margins of the wing are sources from which emanates a wave of morphogen concentration. Murray showed that this simple model could exhibit a wide variety of observed patterns. For example, it exhibits patterns consistent with those observed after microcautery surgery. The theoretical results are consistent with the observation of Schwantwitsch (1924).

By use of a geometrically accurate wing domain, Sekimura *et. al.*, (2000) presented a reaction-diffusion model for the formation of global pigmentation patterns in the butterfly wing of *Papilio dardanus*. The model is based on the idea that a system of reacting and diffusing chemicals can evolve from an initially uniform spatial distribution to concentration profiles that vary spatially—so-called diffusion driven instability (Turing, 1952). By mathematical analysis and computer simulation of the model equations, Sekimura *et. al.*, (2000) suggested that the global wing coloration is essentially due to underlying stripe-like patterns of some pigment inducing morphogen. The generality of the model should allow it to be applied to a wide variety of problems related to wing color patterns.

In the following sections, we review the model framework briefly and then present numerical results which show how the model can be used to make theoretical predictions on cutting experiments.

2. A model for color pattern formation in the butterfly wing of *Papilio dardanus*

Papilio dardanus is a species of butterfly widely distributed across sub-Saharan Africa, and it is well known for its spectacular phenotypic polymorphism in females (see Figure 1). The female wing patterns look very complicated in their appearance and at first glance it seems difficult to find an underlying logical relationship between them even in the single species. However, the work of Nijhout suggests that the black color pattern elements in the wing constitute the principle pattern elements, even though the background color attracts our attention most (Nijhout, 1991). The elements differ in size depending on the mimetic form and this can have dramatic effects on the overall appearance of the pattern (see Figure 2). Our problem is, then, largely

Fig. 1. Polymorphism in mimetic females of *Papilio dardanus*, (i) *trophonius*, (ii) *cenea*, (iii) *planemoides*, (iv) *hippocoonides*.

simplified and our goal is to present a mechanism that can account for only the black pattern elements.

2.1. Model equations

We solve the non-dimensionalised reaction-diffusion system with Gierer-Meinhardt (1972) reaction kinetics

$$u_t = \gamma\left(a - bu + \frac{u^2}{v(1 + ku^2)}\right) + \nabla^2 u, \tag{2.1}$$

$$v_t = \gamma(u^2 - v) + d\nabla^2 v \tag{2.2}$$

using the finite element method on fixed two-dimensional wing domains.   Here $u(\underline{x}, t)$ and $v(\underline{x}, t)$ represent chemical (morphogen) concentrations at spatial position $\underline{x}$ and time t; a, b, d, k and γ are positive parameters.   The following scaling parameters can be derived

$$T = \frac{L_x^2}{D_1}, \qquad \gamma = \frac{k_5 L_x^2}{D_1}, \qquad \text{and} \qquad d = \frac{D_2}{D_1}. \tag{2.3}$$
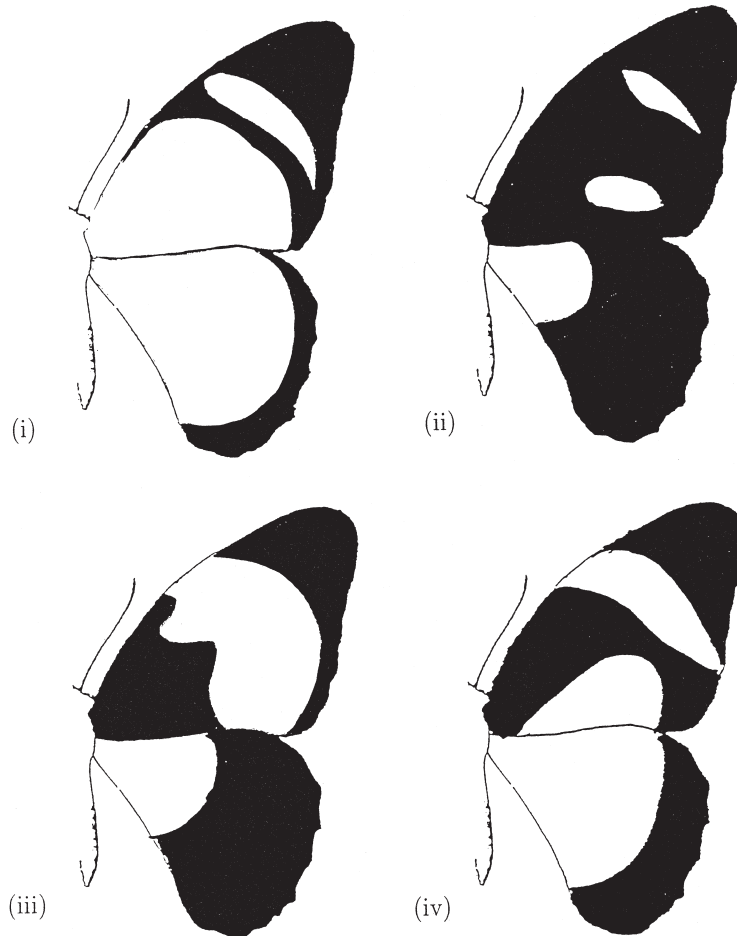
Fig. 2. Diagram illustrating the black pattern elements in mimetic forms of *Papilio dardanus*. (i) *trophonius*, (ii) *cenea*, (iii) *planemoides*, (iv) *hippocoonides*.

L_x is a typical length scale in one dimension (of order *mm* in *Papilio dardanus*), D_1 and D_2 are diffusion coefficients and k_5 is a reaction rate which is characteristic of the reaction kinetics used.

2.2. Numerical simulations

We allow the boundary conditions to take the general form

$$\theta(u - u_1) + (1 - \theta)(u_n - u_2) = u_3 \tag{2.4}$$

with a similar form for v, where u_n is the normal derivative at the boundary

and we impose values on θ, u_1, u_2 and u_3. For example, $\theta = 0$ gives a (Neumann) flux condition, while $\theta = 1$ gives a (Dirichlet) fixed condition. Choosing a value of θ between these extremes results in a mixed (Robin) condition. In the simulations below we also allow θ, u_1, u_2 and u_3 to be functions of position along the boundary. We assume that patterning occurs across the whole domain but is locally controlled by different types of boundary conditions (for example, see the boundary conditions illustrated in Figure 6).

For illustrative purposes we fix the values of $a = 0.1$, $b = 1.0$ and $k = 0.5$, while the values of γ and d are determined from the Turing space according to the mode which would be selected on particular regular domains with zero-flux boundary conditions, for which standard linear analysis can be carried out. The numerical simulations show the plots of v only. The profiles of u can easily be deduced from these plots as they are in phase with those of v (for more details, see, Madzvamuse, 2000).

The standard application of Turing models in developmental biology assumes that there is a fixed constant concentration threshold so that cells that experience a morphogen concentration above this threshold will differentiate, while those that experience a lower morphogen concentration remain undifferentiated. In all the simulations in this paper, we assume that cells within the wing are not necessarily homogeneous in their response to one of the chemical concentrations, in this case v. We therefore allow the threshold function to take the more general form of a plane $\alpha y + \beta x + c_0$ where α or β or both are non-zero and c_0 is a non-negative constant. Here coloration or shading is determined as follows: if cells experience chemical concentration $v \geq \alpha y + \beta x + c_0$ they are black, otherwise they become colored. That is, we assume that sufficiently high concentrations of v stimulate cells to produce pigment. Note that if both α and β are zero, then the threshold gradient is reduced to a constant threshold, while if one of α or β is zero, then cells are homogeneous in one direction but have a response gradient in the other direction. There is no biological evidence to justify the existence of a gradient threshold. However, there is experimental evidence (Sekimura $et.$ $al.$, 1998, 1999) that cells do have other properties, such as adhesivity, which depend on distance from the body. The threshold parameters are taken to be $\alpha = -0.111$, $\beta = -0.025$ for the forewing, while for the hindwing $\alpha = 0.111$, $\beta = -0.025$. The gradient threshold values are determined by trial and error. The forewing and hindwing domains are considered independent, hence numerical simulations are carried out on each domain separately. With the kinetic parameters fixed as above, we further select the values $d = 70.8473$ and $\gamma = 619.45$, chosen to select the $(3, 0)$ mode with zero flux boundary conditions on a unit square. The uniform homogeneous steady state is linearly unstable to this mode for these parameter values. These values are used in the simulations shown in

Figures 3, 5 and 7. We take initial conditions as small random perturbations about the uniform homogeneous steady state.

3. Results

The numerical method we used is detailed in Madzvamuse (2000). Here, we simply present a selection of numerical results, which also show the mesh we used for our finite element simulations (Figures 3–7).

3.1. Mimetic forms

Comparing Figure 2 with our numerical simulations (Figure 3) we see that a simple reaction-diffusion model can capture the details of the differ-
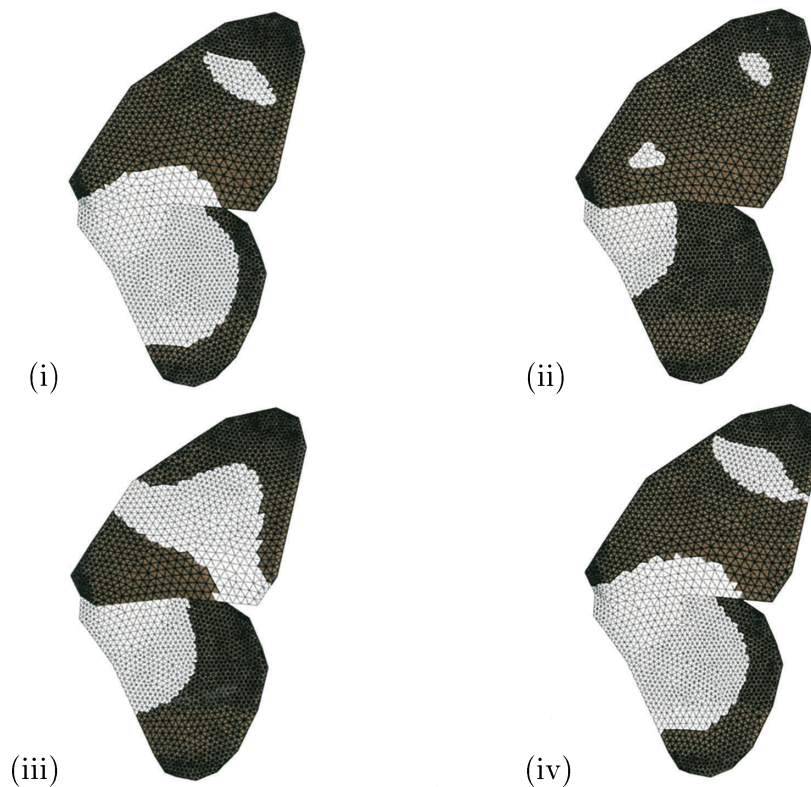
Fig. 3. Results of numerical simulations of the Gierer-Meinhardt model (2.1)–(2.2). For comparison with *Papilio dardanus* see Figure 1. Mimetic forms: (i) *trophonius*, (ii) *cenea*, (iii) *planemoides* and (iv) *hippocoonides*. Black indicates concentrations of v above the threshold gradient, white indicates values below the threshold gradient. Model and threshold parameters are given in Table 1, boundary conditions are shown in Figure 4.

Table 1: Parameter values and gradient threshold values used in the numerical simulations in Figure 3.

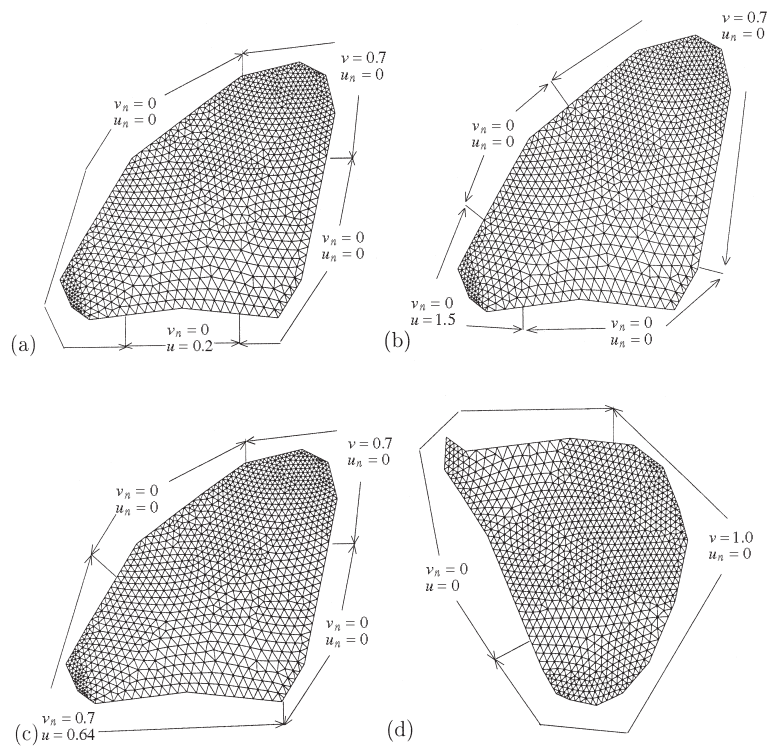| Pattern	Forewing	Hindwing
trophonius	$d = 70.8473$, $\gamma = 619.45$ $\alpha = -0.111$, $\beta = -0.025$, $c_0 = 0.697$	Same as forewing except $\alpha = 0.111$, $\beta = -0.025$ $c_0 = 0.9$
hippocoonides	Same as for *trophonius* except $c_0 = 0.701$	$c_0 = 0.87$
planemoides	Same as for *trophonius* except $c_0 = 0.67$	$c_0 = 0.7$
cenea	Same as *trophonius* except $\alpha = -0.0111$, $\beta = -0.025$, $c_0 = 0.653$	$c_0 = 0.6$

Fig. 4. Boundary conditions for the simulations shown in Figure 3. Forewings of (a) *trophonius*, *hippocoonides*, (b) *planemoides*, (c) *cenea*. (d) Hindwing (all butterflies).
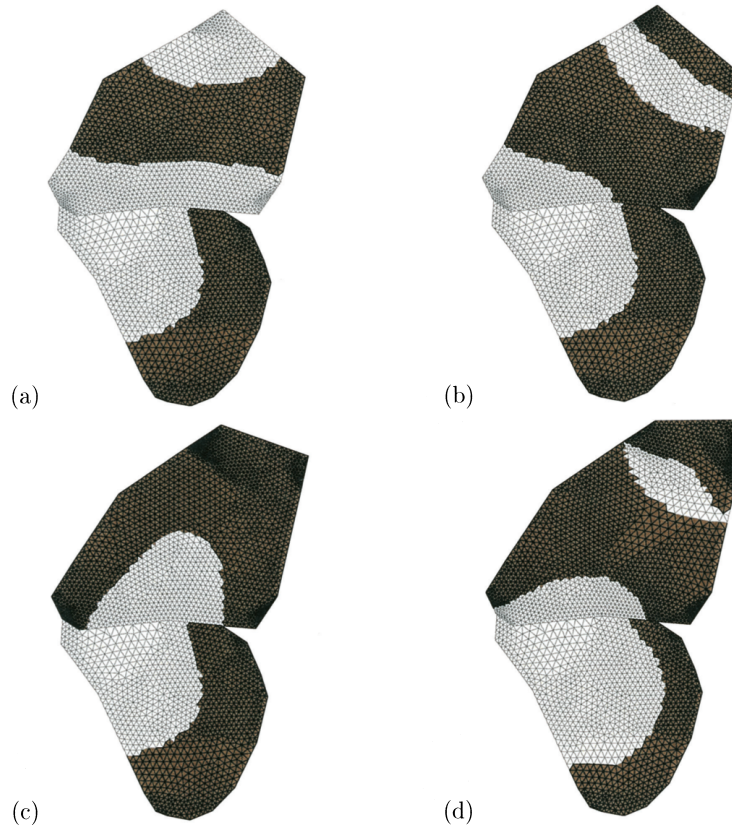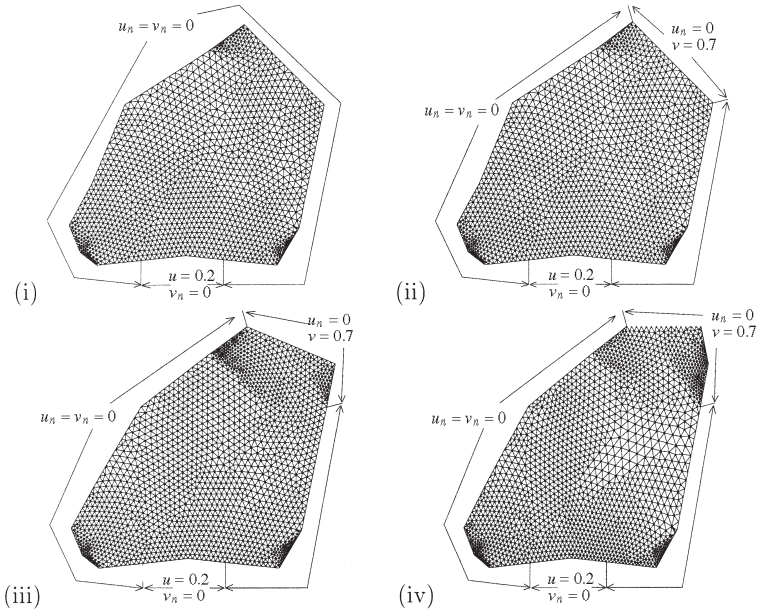
Fig. 5. Model predictions on the effects of cutting the forewing of *Papilio dardanus hippocoonides*. Compare results with simulations for *hippocoonides* in Figure 3. Corresponding boundary conditions are shown in Figure 6. Here $c_0 = 0.701$.

ent patterns. In these simulations, the parameter values $\alpha = -0.111$ and $\beta = -0.025$ are fixed for the threshold function in the forewing patterns in *hippocoonides, planemoides, trophonius* and *cenea*. For the hindwing the same numerical values are taken except that α has positive sign. With these values, we find that the forewing patterns for *hippocoonides* and *trophonius* are generated with the same boundary conditions and with very small changes in c_0 (Figure 4).

Our numerical simulations reveal that only small changes in threshold are necessary to determine different observed patterns. For example, the forewing patterns of the *hippocoonides* and *trophonius* are obtained from the same boundary conditions and parameter values with less than 0.1% change in the threshold. We also find that the boundary conditions play a crucial role in

Fig. 6. Boundary conditions for the numerical simulations shown in Figure 5 (a), (b), (c) and (d) respectively.
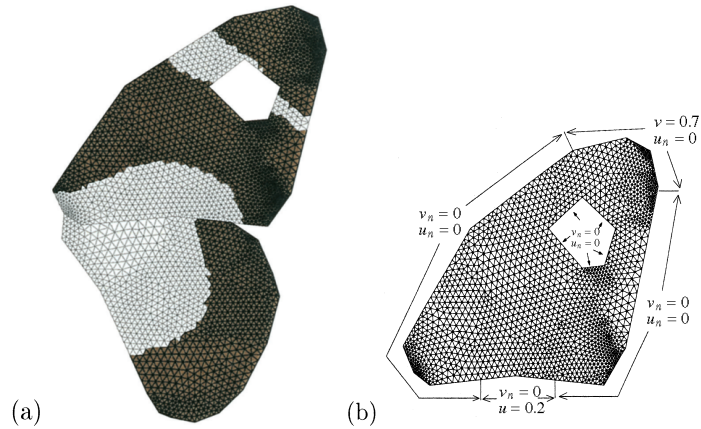
Fig. 7. (a) Model predictions on the effects of making a hole in the wing of *hippocoonides*. Compare results with simulations for *hippocoonides* in Figure 3. (b) Shows the boundary conditions used to simulate the forewing pattern in (a). Zero-flux boundary conditions are imposed around the hole.

orientation of pattern. A large number of wing patterns can be simulated with the same boundary conditions. The hindwing appears to admit more simple patterns, consistent with the observations in Figure 1. These are simulated with the same model parameter values as used for the forewing. The boundary conditions on the hindwing are shown in Figure 4 and are unchanged for the different simulations. These simulations show that the variety of patterns exhibited by *Papilio dardanus* can be obtained under tight control of only a few parameters.

3.2. Effects of cutting part of the forewing

To illustrate the predictive power of our model, we now simulate the effects of a cutting experiment by simply removing part of the patterning domain and imposing a zero-flux boundary condition on the newly generated boundary, while keeping the conditions on the other parts of the boundary unchanged.

In Figure 5 (a) we show the results of a simulation in which the boundary conditions on the intact edges are those we used in the simulations for *hippocoonides* (Figure 4 (a)), while zero-flux boundary conditions are imposed along the cut edge. It can be seen that assuming these are the appropriate boundary conditions for the cut edge results in a pattern that is very different to the normal pattern. However, if we impose on the cut edge the original boundary conditions, we obtain a pattern more similar to the normal pattern (Figure 5 (b)). For these boundary conditions the effects of different sized cuts are shown in Figure 5 (c) and (d).

3.3. Effects of making a hole

Figure 7 shows numerical results simulating the effects of making a hole in the forewing. In these simulations, zero-flux boundary conditions are assumed along the boundaries of the hole while the external boundary conditions remain unchanged from those used to simulate normal development. According to our results, making a hole on the *hippocoonides* forewing domain appears not to have a major effect on pattern formation.

4. Discussion

We have shown that a reaction-diffusion system solved on a realistically shaped adult wing geometry for *Papilio dardanus* can produce the variety of mimetic (and non-mimetic) pigmentation forms observed under tight control of only a few parameters. We have shown how the model can be used to make predictions on the outcome of cutting experiments. In certain cases, our model

predicts that cutting experiments will have a global effect. This is in contrast to the model of Nijhout (1991), which assumes that the different forms observed in *Papilo dardanus* forewings are due to different growth dynamics of four subdomains within the domain. In that case, cutting experiments would have only a local effect. Although we have only shown results for *hippocoonides* our model can obviously be used in a similar fashion to predict the outcome of cutting experiments for the other forms.

It should be noted that by simulating our model on the adult wing we are implicitly assuming that pigment pattern formation occurs in the adult. However, it is probably the case that the pigmentation process occurs earlier. We are presently carrying out numerical simulations for realistically growing domains to investigate this issue.

We have assumed that there are sources and sinks of chemicals at various parts on the boundary and therefore have simulated cut boundaries by zero-flux conditions (assuming that any sources or sinks have been destroyed). However, the healing process may in fact result in the growth of new tissue and the regeneration of these sources and sinks. Our simulations show that the latter assumption results in very different predictions to those for the former assumption. We aim to explore this issue in future theoretical and experimental studies.

Acknowledgements

References

[1] Gierer, A. and Meinhardt, H. (1972). A theory of biological pattern formation. Kybernetik, **12**: 30–39.

[2] Kühn, A. and Von Engelhardt, A. (1933). Über die determination des symmetrie systems auf dem vorderflügel von phylogeny, Evolution, **42**: 862–884.

[3] Madzvamuse, A. (2000). A Numerical Approach to the Study of Spatial Pattern Formation. D Phil Thesis, University of Oxford.

[4] Meinhardt, H. (1982). Models of Biological Pattern Formation. Academic Press, New York.

[5] Müller, J. D.; Roe, P. L. and Deconinck, H. (1993). A frontal approach for internal node

generation for Delaunay triangulations, Int. J. of Num. Meth. in Fluids, Vol. **17**: No. **3**, 241–56.

[6] Murray, J. D. (1981). On pattern formation mechanisms for lepidopteran wing patterns and mammalian coat markings, Phil. Trans. Roy. Soc. Lond., **B 295**: 473–496.

[7] Murray, J. D. (1993). Mathematical Biology. Heidelberg New York, Springer-Verlag.

[8] Nijhout, H. F. (1990). A comprehensive model for colour pattern formation in butterflies, Proc. Roy. Soc. Lond., **B 239**: 81–113.

[9] Nijhout, H. F. (1991). The Development and Evolution of Butterfly Wing Patterns. Smithsonian Institution Press, Washington and London.

[10] Nijhout, H. F. (1994). Genes on the wing, Science, **265**: 44–45.

[11] Schwanwitsch, B. N. (1924). On the ground plan of wing-pattern in nymphalids and certain other families of rhopalocerous Lepidoptera, Proc. Zool. Soc. Lond., ser **B 34**: 509–528.

[12] Sekimura, T.; Maini, P. K.; Nardi, J. B.; Zhu M. and Murray, J. D. (1998). Pattern formation in lepidopteran wings, Comments Theor. Biol., **5**: No. 2–4, 69–87.

[13] Sekimura, T.; Zhu, M.; Cook, J.; Maini, P. K. and Murray, J. D. (1999). Pattern formation of scale cells in lepidoptera by differential origin-dependent cell adhesion, Bull. Math. Biol., **61**: 807–827.

[14] Sekimura, T.; Madzvamuse, A.; Wathen, A. J. and Maini, P. K. (2000). A model for colour pattern formation in the butterfly wing of *Papilio dardanus*, Proc. Roy. Soc. Lond. **B 267**: 851–859.

[15] Süffert, F. (1927). Zur vergleichende analyse der schmetterlingszeichung, Biologisches zentralblatt **47**: 385–413.

[16] Turing, A. M. (1952). The chemical basis of morphogenesis, Phil. Trans. Roy. Soc. Lond. **B 237**: 37–72.

Anotida Madzvamuse
Oxford University Computing Laboratory
Wolfson Building
*Parks Road, Oxford OX*1 3*QD, UK*

Philip K. Maini
Centre for Mathematical Biology
Mathematical Institute
University of Oxford
24-29 *St Giles', Oxford OX*1 3*LB, UK*

Andrew J. Wathen
Oxford University Computing Laboratory
Wolfson Building
*Parks Road, Oxford OX*1 3*QD, UK*

Toshio Sekimura
Department of Biological Chemistry
College of Bioscience and Biotechnology
Chubu University
Kasugai, Aichi 487-8501, *Japan*